Archival Report

Biological Psychiatry: Celebrating 50 Years

The Relative Contributions of Cell-Dependent Cortical Microcircuit Aging to Cognition and Anxiety

Rammohan Shukla, Thomas D. Prevot, Leon French, Ruth Isserlin, Brad R. Rocco, Mounira Banasr, Gary D. Bader, and Etienne Sibille

ABSTRACT

BACKGROUND: Aging is accompanied by altered thinking (cognition) and feeling (mood), functions that depend on information processing by brain cortical cell microcircuits. We hypothesized that age-associated long-term functional and biological changes are mediated by gene transcriptomic changes within neuronal cell types forming cortical microcircuits, namely excitatory pyramidal cells (PYCs) and inhibitory gamma-aminobutyric acidergic neurons expressing vasoactive intestinal peptide (*Vip*), somatostatin (*Sst*), and parvalbumin (*Pvalb*).

METHODS: To test this hypothesis, we assessed locomotor, anxiety-like, and cognitive behavioral changes between young (2 months of age, $n = 9$) and old (22 months of age, $n = 12$) male C57BL/6 mice, and performed frontal cortex cell type–specific molecular profiling, using laser capture microscopy and RNA sequencing. Results were analyzed by neuroinformatics and validated by fluorescent in situ hybridization.

RESULTS: Old mice displayed increased anxiety and reduced working memory. The four cell types displayed distinct age-related transcriptomes and biological pathway profiles, affecting metabolic and cell signaling pathways, and selective markers of neuronal vulnerability (*Ryr3*), resilience (*Oxr1*), and mitochondrial dynamics (*Opa1*), suggesting high age-related vulnerability of PYCs, and variable degree of adaptation in gamma-aminobutyric acidergic neurons. Correlations between gene expression and behaviors suggest that changes in cognition and anxiety associated with age are partly mediated by normal age-related cell changes, and that additional age-independent decreases in synaptic and signaling pathways, notably in PYCs and somatostatin neurons, further contribute to behavioral changes.

CONCLUSIONS: Our study demonstrates cell-dependent differential vulnerability and coordinated cell-specific cortical microcircuit molecular changes with age. Collectively, the results suggest intrinsic molecular links among aging, cognition, and mood-related behaviors, with somatostatin neurons contributing evenly to both behavioral conditions.

Keywords: Aging, Anxiety, Canonical microcircuit, Cognitive deficit, Neuronal vulnerability, Ontology, Single cell–type RNAseq

https://doi.org/10.1016/j.biopsych.2018.09.019

Age-related changes in cognitive and mood-related functions are thought to be mediated by subtle structural and functional changes in various brain regions and at the cell level by adaptations in cortical microcircuits mediating information processing (1). In a simplified model of cortical microcircuitry, excitation mediated by glutamatergic pyramidal cells (PYCs) undergoes an orchestrated modulation by distinct gamma-aminobutyric acid (GABA)–expressing inhibitory neurons (2,3). Specifically, *Sst*-expressing GABAergic (SST) neurons inhibit PYC dendrites; *Vip*-expressing GABAergic (VIP) neurons inhibit SST neurons, hence, together with SST neurons, regulating excitatory input onto PYCs. *Pvalb*-expressing GABAergic (PV) neurons target the PYC perisomatic region, hence regulating excitatory output. The balance of activities between PYC and GABAergic neurons, often referred to as excitation-inhibition (E/I) balance, significantly contributes to microcircuit, brain region, and neural network homeostasis, which then determines the content, integrity, and transfer of information flowing through these biological levels (4,5). Conversely, age-related long-term cell-dependent changes occur in a coordinated manner to maintain microcircuit homeostasis, which, in turn, are thought to underlie age-associated behavioral and cognitive changes.

With age, glutamatergic (6) and GABAergic (7) transmission is altered, leading to changes in synaptic input/output, plasticity, and neuronal excitability (8). The area and cell-type specificity of these changes can be associated with neuronal vulnerabilities with age, which alter functional adaptations and E/I balance (9). Much has been learned about short-term

SEE COMMENTARY ON PAGE 187

ISSN: 0006-3223

(seconds to hours) functional adaptations at the cell contact level; however, how the different cell types of those microcircuits synchronize their functions on longer timescales (weeks to months) is less well known. Long-term biological adaptations are specifically relevant to age-associated brain changes. Hence, we hypothesize that age-associated decline in long-term homeostatic changes is regulated through coordinated transcriptional programs within and across cell types forming cortical microcircuits.

To begin testing this hypothesis, we first assessed changes in behavior and cognitive abilities in young and aged mice and performed frontal cortex cell type–specific molecular profiling, using laser capture microscopy (LCM) and RNA sequencing (RNAseq). Behavioral and molecular results were analyzed for coordinated changes using ontological analysis approaches. We predicted that 1) age-, anxiety-, and cognition-related biological changes would differ across microcircuit cell types; and 2) PYC changes would be accompanied by inversely correlated changes among VIP, SST, and PV GABAergic neurons, to maintain homeostasis through regulating excitatory input and output onto PYCs. Finally, we sought evidence for a potential order in cell-dependent vulnerability to age-related changes as a first step toward investigating the putative sequence of cell-dependent events underlying brain aging.

METHODS AND MATERIALS

Detailed methods are available in Supplement 1.

Animals

All experiments were performed with male C57BL/6 mice 22 (n = 12) and 2 (n = 9) months of age in accordance with the Canadian Animal Care Committee and in the order described in Figure 1A.

RNA Extraction and Sequencing Library Preparation

After tissue sectioning, staining, and laser capture steps, the RNA from the microdissected cells were extracted using the PicoPure RNA Isolation kit (Cat. No. KIT0204; Thermo Fisher Scientific, Waltham, MA), and libraries were prepared using the SMARTer RNASeq pico input kit (Cat. No. 635007; Clontech Laboratories, Mountain View, CA), according to the manufacturer protocols, and were sequenced using the Illumina HiSeq 2500 (Illumina, Inc., San Diego, CA) to generate 2 × 100 paired-end reads.

Differential Expression Analysis

The reads were aligned to mouse reference genome GRCm38 using HISAT2 aligner (https://ccb.jhu.edu/software/hisat2/index.shtm), and counts were generated and analyzed for differential expression using Deseq2 (10). A p value $< .05$ was used to select differential expressed genes. For gene-behavior correlations, we performed Spearman correlation of anxiety and cognition Z-scores with DESeq2-normalized gene expression, from which the age-associated residuals were subtracted.

Pathway Analysis

The Wald statistics–based ordered list of genes for the effect of age in different cell types was used to map the enrichment

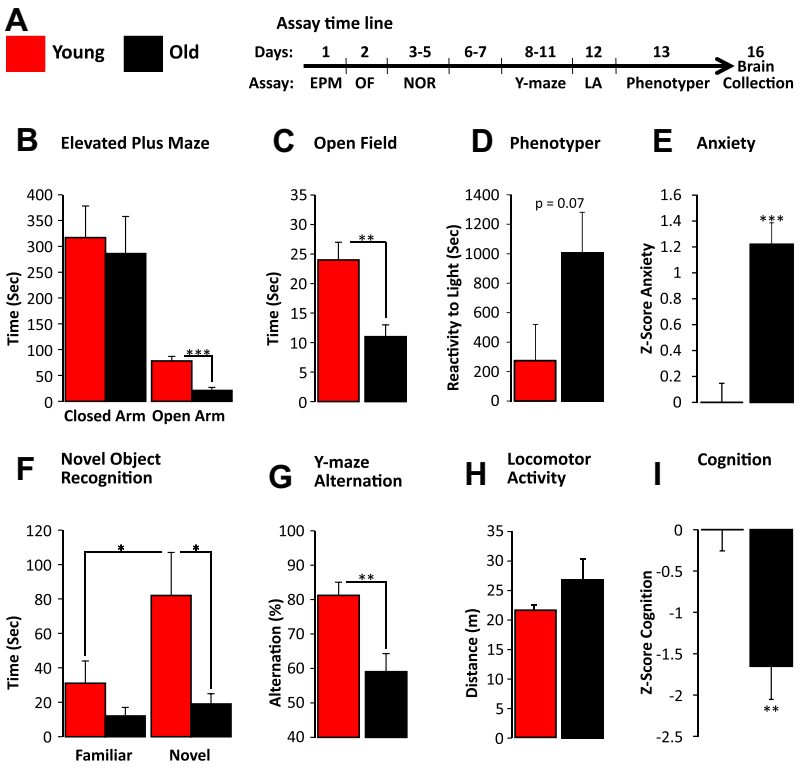

Figure 1. Age-related behavioral changes. **(A)** Timeline of assays conducted in the study. Results are summarized for **(B–E)** anxiety-like behavior, **(F, G)** cognitive deficits, and **(H)** locomotor activity (LA) changes in young (red, n = 9) and old (black, n = 12) mice. **(B)** Anxiety-like behavior was assessed in the elevated plus maze (EPM). Old animals spent less time in open arms, whereas there was no difference in the closed arm. **(C)** Old animals spent less time in the center of the open field (OF) than young animals. **(D)** There was a near-significant difference in the reactivity to a light challenge in the PhenoTyper, with a potential higher reactivity in old animals compared with young animals, together **(B–D)** demonstrating increased anxiety-like behaviors in old mice, as summarized by the Z-score in panel **(E)**. **(F)** The time spent around the familiar and novel objects in the novel object recognition (NOR) test was assessed. Results showed reduced time spent around the novel object in old mice compared with young mice. **(G)** Aged animals showed a deficit in working memory characterized by decreased alteration rate in the Y-maze test. **(H)** Both young and old animals showed no changes in locomotor activity with age. **(I)** The Z-score of the cognition-associated behaviors is shown in panels **(F)** and **(G)**. $^{*}p < .05$; $^{**}p < .01$; $^{***}p < .001$.

of different gene ontology terms in the biological pathway, molecular function, and cellular component categories, using default gene set enrichment analysis parameters (11). An updated list of Gene Ontology (GO) terms was downloaded (http://download.baderlab.org/EM_Genesets/). To analyze age effects across cell types, the normalized enrichment score of significant pathways (p value $<$ .05) was used. Custom R-script written in R version 3.4.0 (R Foundation for Statistical Computing, Vienna, Austria) and GODB package (https://bioconductor.org) was used to explore the parent–child association between GO terms in our list of significant pathways (child pathways) and handpicked pathways in GO database (parent pathway), representing known changes in aging.

Quantitative Microscopy

For validation of differential expression and neuronal vulnerability analyses, we counted the fluorescent in situ hybridization (FISH)–labeled messenger RNA grains using quantitative widefield microscopy and FISH-quant (12) in MATLAB 9.2 (R2017a) (The MathWorks, Inc., Natick, MA).

RESULTS

Anxiety-like and Cognitive Behaviors in Old Versus Young Mice

Old mice spent significantly less time in the open arms of the elevated plus maze compared with young mice (Figure 1B) ($p < .001$), with no difference in time spent in the closed arms of the maze ($p = .76$). In the open field test, old mice spent less time in the center of the apparatus (Figure 1C) ($p = .002$). Finally, in home cage–like settings using the PhenoTyper (Noldus, Leesburg, VA), old mice exposed to an anxiogenic light stimulus displayed exacerbated reactivity compared with young mice (Figure 1D) ($p = .07$). Together these results demonstrate higher anxiety-like behaviors in old compared with young animals, as confirmed by averaged transformed Z-scores across tests (t test, $p < .0001$) (Figure 1E).

Cognitive functions were tested using the novel object recognition test and spatial alternation in a Y-maze. In the novel object recognition (Figure 1F), analysis of variance revealed an effect of age ($F_{1,19} = 6.8$, $p = .02$), an effect of the type of object ($F_{1,19} = 8.9$, $p = .007$), and an interaction between both factors ($F_{1,19} = 5.5$, $p = .03$). Post hoc analysis revealed that young animals explored the novel object more than the familiar one ($p = .05$), whereas old animals did not ($p = .43$). Also, old animals explored the novel object less than young animals ($p = .014$). In the Y-maze (Figure 1G), the spontaneous alternation rate was low in old mice compared with young mice ($p = .005$). There was no difference in locomotor activity (Figure 1H) between young and old animals ($p = .2$). Together, these results demonstrate reduced cognitive functions in old compared with young animals, as confirmed by averaged transformed Z-scores across tests ($p = .0047$) (Figure 1I).

Cortical Microcircuit Cell Types Display Unique and Minimally Overlapping Age-Related Transcriptomic Profiles

To investigate the cellular and molecular correlates of age-related behavioral changes, we collected the four cell types forming canonical cortical microcircuits (PYC, PV, SST, and VIP GABAergic neurons) (Figure 2A) in the frontal cortex of the same mice using FISH and LCM (Figure 2B), and obtained cell-specific gene expression profiles using RNAseq. The reads from the four cell types mapped to 13,986 genes. A principal component analysis showed a clear separation of cell types in unique clusters (Figure 2C), demonstrating distinct patterns of gene expression for each cell type. Cell type markers (*Slc17a17*, *Sst*, *Pvalb*, and *Vip*) displayed the expected levels of expression enrichment (Figure 2D). Moreover, all cells expressed *Stmn2*, a pan-neuronal marker, whereas *Gad1 and Gad2*, two interneuron-specific markers, were expressed exclusively in GABAergic neurons (Figure 2D), together validating the cell collection approach.

Next, we investigated age-related changes in gene expression within and across cell types. No genes were significantly affected across the four cell types at the 10% false discovery threshold (false discovery rate; $q < 0.1$). In contrast, 7.9% of genes were affected in at least one cell type at the same threshold. In order of magnitude, VIP neurons have the highest number of differentially expressed genes, followed by PYC neurons, and PV/SST neurons (Figure 2E). Age-downregulated genes were more common than upregulated genes in VIP cells and PYCs and equivalent in SST and PV cells (Figure 2E). Overlaps in expression profiles were minimal between cell types (Figure 1F, G).

Next, we explored the biological pathways associated with differentially expressed genes in each cell type using gene set enrichment analysis. Few pathways were identified at false discovery rate < 0.25 (PV: 0 down and 4 up, SST: 7 down and 0 up, VIP: 10 down and 0 up), except for PYC neurons (142 down and 48 up), suggesting weaker age-associated changes in interneurons. Thus, for further analysis, we focused on pathways identified at $p < .05$. PYCs had the highest number of significantly affected pathways, and PV neurons the least, and except for some degree of overlap in enriched synapse-associated pathways between VIP and PYC neurons (Table S1 in Supplement 2), there was minimal overlap in affected pathways across cell types (Figure 3A).

Cell-Dependent Metabolic and Synaptic Aging

To further investigate cell-dependent aging, we utilized the hierarchical GO tree structure (13) and selected two sets of GO parent terms, one associated with metabolism and cellular stress and the other associated with synaptic homeostasis and channel activity reflecting the neuronal E/I balance, as two hallmarks of biological aging (14). We then filtered the cell-specific distribution of affected biological pathways (child terms) associated with these parent terms. Results are summarized in Figure 3B and below per cell type.

Pyramidal Cells. PYCs showed prominent downregulation in the GO term response to stress pathways (9 of 33 child terms) (Figure 3B; Table S2 in Supplement 2) and upregulated pathways related to oxidation-reduction process, leading to the generation of reactive oxygen species (6 of 8 terms). Pathways associated with energy production (ATP metabolic process), organelles activity (mitochondrion, lysosome, and endoplasmic reticulum), cellular response to DNA damage

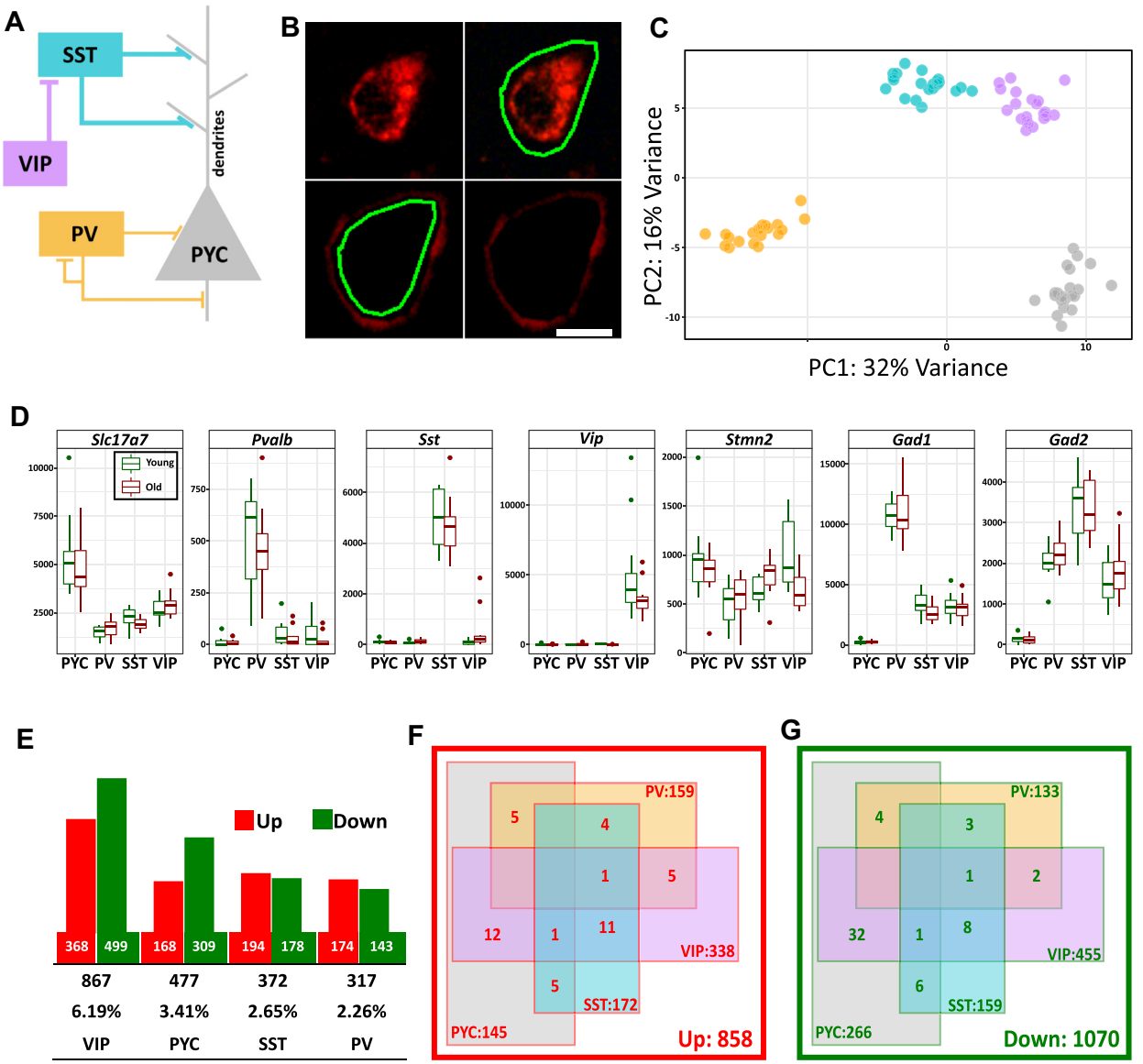

Figure 2. Cell-specific analysis of age-related differential gene expression. **(A)** Canonical cortical-microcircuit containing pyramidal cell (PYC), parvalbumin (PV), somatostatin (SST), and vasoactive intestinal peptide (VIP) neurons. The color labels used for different neurons in panel **(A)** are maintained for all the figures. **(B)** Cells are labeled with RNAscope fluorescent in situ hybridization and collected by laser capture microdissection. Scale bar = 10 μm. **(C)** A transcriptome-based principal component (PC) analysis plot clearly showed distinct neuronal cell–type clusters. **(D)** Validation of cell-type collection: Markers of cell types show expected cell-specific expression. **(E)** Number of age-related differentially expressed genes per cell type ($p < .05$). Percentage values correspond to 13,986 genes analyzed. **(F, G)** Overlap of differentially expressed gene between cell types in the **(F)** upregulated and **(G)** downregulated conditions.

stimulus, and proteolysis (protein ubiquitination and protein catabolic process) were also upregulated with age, suggesting that the energy produced is consumed in cellular maintenance. In contrast, there was a prominent downregulation of a pathway associated with synaptic signaling (11 of 21 terms) and synapse part (8 of 10 terms), mostly including excitatory synapse (modulation of excitatory postsynaptic potential) (Table S2 in Supplement 2). Other subcellular anatomy–related pathways, namely axon development, dendrite development, cell junction organization (exclusive for PYCs), and cytoskeleton organization, were similarly downregulated in PYCs. For channel activities, there was a small upregulation of ATPase activity (2 of 10 terms), and downregulation of voltage-gated channel activities that include calcium gated channels (1 of 7 terms) and potassium gated channels (1 of 7 terms). Finally, cation homeostasis pathways were exclusively downregulated in PYCs. Together, this suggests an age-related functional shift in PYCs toward increased cellular stress and metabolism and reduced signaling functions during aging.

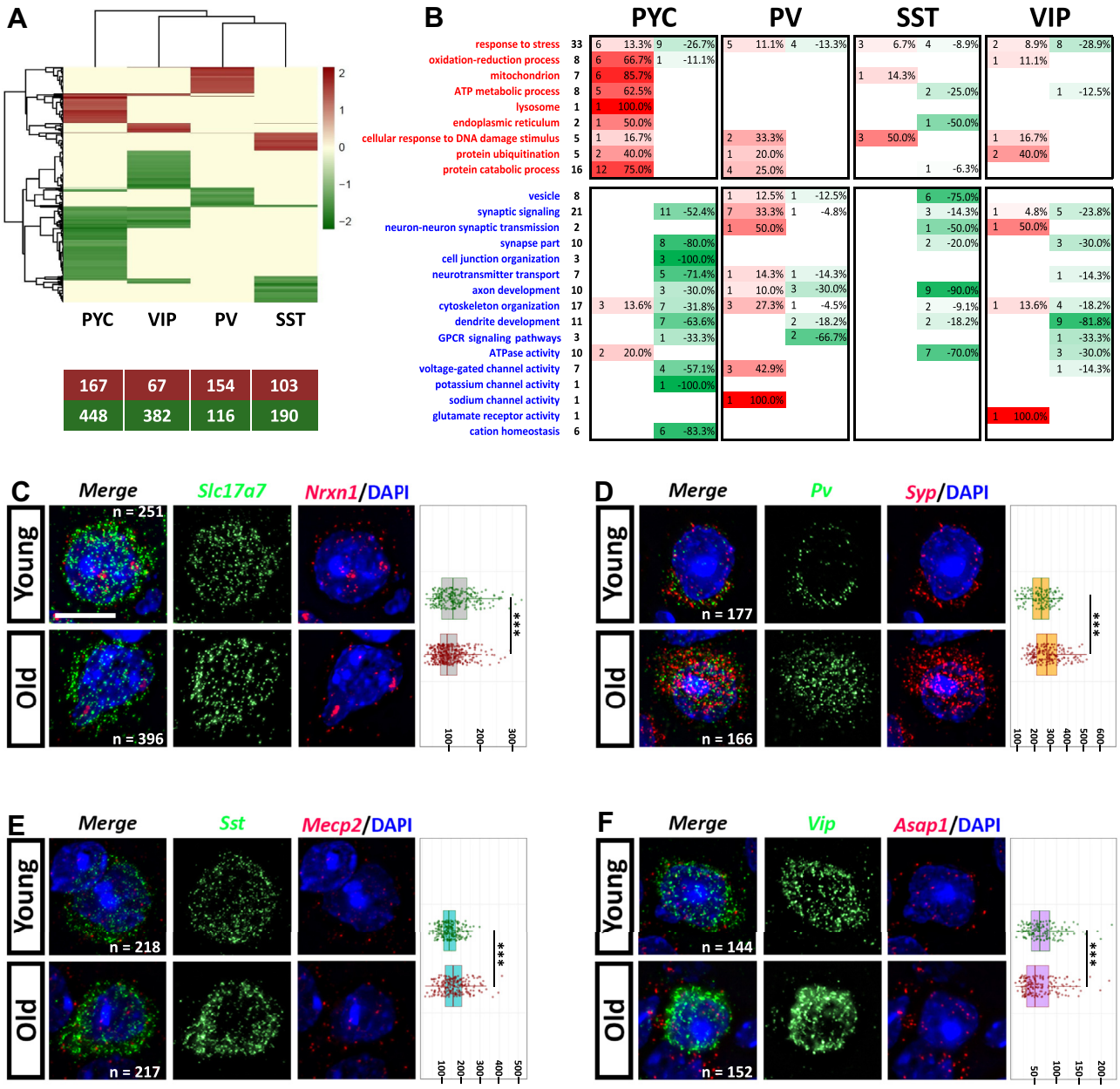

Figure 3. Cell-dependent age-related affected biological pathways and validation of differential expression of associated markers. **(A)** Clustering of age-affected biological pathways in pyramidal cell (PYC), vasoactive intestinal peptide (VIP), parvalbumin (PV), and somatostatin (SST) neurons ($p < .05$). Each row (nodes of the dendrogram on the left) represents a pathway and each column a cell type. The scale represents the normalized enrichment score for upregulated (red) and downregulated (green) pathways. The numbers below represent upregulated and downregulated pathways per cell type. Refer to Table S1 in Supplement 2 for a complete list of pathways associated with each cell type and pathway overlap between cell types. **(B)** Altered pathways related to metabolism and cellular stress (top, red) and synaptic homeostasis and channel activity (bottom, blue), per cell type. The pathway names on the left represent the parent terms selected from the Gene Ontology (GO) database and their associated child term (black numbers). On the right, the red and green colors represent upregulated and downregulated numbers of pathways per cell type, respectively, scaled to the total percent of child term associated with the parent term per cell type. Refer to Table S2 in Supplement 2 for the detailed parent–child associations with respect to age FISH-quant validation of genes representative of affected GO groups: **(C)** *Nrxn1*, belonging to the GO group presynaptic active zone, downregulated with age in PYCs; **(D)** *Syp*, belonging to the GO group regulation of long-term neuronal plasticity, upregulated with age in PV neurons; **(E)** *Mecp2*, belonging to the GO group negative regulation of gene expression, upregulated with age in *Sst* neurons; **(F)** *Asap1*, belonging to the GO group dendritic spine morphogenesis, downregulated with age in VIP neurons. Messenger RNA grains were counted for the differentially expressed genes (red in right columns), based on cells selected using *Slc17a7*, *Pvalb*, *Sst*, *and Vip* markers (green in middle columns). The boxplots of messenger RNA counts are displayed per gene on the right. Axis is in grains per cell. "n" in the merged figure represents the number of cells investigated. ***$p < .001$. Scale bar = 10 μm. ATP, adenosine triphosphate; GPCR, G protein–coupled receptor.

PV Neurons. Upregulated pathways were more abundant than downregulated pathways. Pathways associated with oxidation-reduction process, ATP metabolic process, and associated organelles were not changed, but pathways associated with cellular response to DNA damage stimulus (2 of 6 terms) and protein catabolic process (4 of 16 terms) were upregulated. Similarly, pathways associated with synaptic changes showed greater up- than downregulation with age. PV neurons showed the highest proportion of upregulated child terms associated with synaptic signaling (7 of 21 terms), including regulation of synaptic glutamatergic transmission, positive regulation of long-term synaptic potentiation, and modulation of excitatory postsynaptic potential (Table S2 in Supplement 2). Downregulated pathways were associated with axon development (3 of 10 terms) and dendrite development (2 of 11 terms) and with GPCR (G protein–coupled receptor) signaling pathways (2 of 3 terms). For channel activity, PV neurons showed upregulated pathways associated with voltage-gated channel activity, including regulation of postsynaptic membrane potential, sodium channel activity, and calcium channel activity (Table S2 in Supplement 2). Together, this suggests that PV neurons undergo a balanced cellular organization at the metabolic and cell signaling levels to maintain functional homeostasis, without any obvious overall deleterious effect during aging.

SST Neurons. Downregulated pathways were more abundant than upregulated pathways. Upregulated pathways were associated with metabolic changes, including response to stress (3 of 33 terms), mitochondrion (1 of 7 terms) and cellular response to DNA damage stimulus (3 of 6 terms). Downregulated pathways included response to stress (4 of 33 terms), ATP metabolic process (2 of 8 terms), endoplasmic reticulum related activity (1 of 2 terms), and protein catabolic process. Interestingly, the four downregulated child terms associated with response to stress include GO Biological Process pathways associated with kinase activity, stress-activated MAPK cascade, stress-activated protein kinase signaling cascade, and regulation of JUN kinase activity (Table S2 in Supplement 2). In contrast to metabolic changes, all pathways associated with synaptic changes were downregulated in SST neurons, including vesicle, synapse part, neurotransmitter transport (including GABAergic transmission, axon development, and dendrite development) (Figure 3B; Table S2 in Supplement 2). Vesicle and axon development showed highest numbers of downregulated child terms in SST compared with all other neurons. Finally, pathways associated with G protein receptors and channel activities were mostly unaffected. Together this suggests a downregulation of metabolic activities and robust decreases in signaling structure and function in SST neurons with age.

VIP Neurons. VIP neurons showed the most downregulated child terms associated with response to stress (8 of 33) and upregulated pathways related to oxidation-reduction process (1 of 8) among neuron subtypes. Pathways associated with response to DNA damage stimulus (1 of 6 terms) and protein ubiquitination (2 of 5 terms) were upregulated. Among the pathways associated with synaptic changes, there was a downregulation of pathways associated with synaptic signaling (5 of 21 terms) and synapse part (3 of 10 terms), which are proportionately more numerous than for the other two interneuron subtypes. Similarly, there was a greater downregulation of child term pathways associated with dendrite development compared with the other interneuron subtypes. Within channel activities, ATPase activity (3 of 10 terms) and voltage-gated activity (1 of 7 terms) were downregulated, but the pathway associated with glutamate receptor activity was exclusively upregulated in these neurons. Overall, VIP neurons showed similarities with altered pathways identified in PYC neurons (Figure 3A). Together, this suggests a mixed homeostatic adaptation to cellular stress and a functional downregulation of VIP neurons with age, which parallels those observed in PYC neurons.

Validation of Altered Gene Expression by FISH

To validate the RNAseq findings, we selected differentially expressed genes among the core sets of transcripts that account for the enrichment signal (i.e., leading-edge subset) (12) in the four different cell types and performed FISH and quantification by FISH-quant. We confirm that in PYC neurons, neurexin1 (*Nrxn1*), a cell surface receptor associated with the GO term presynaptic active zone, is downregulated with age (RNAseq: $p < .0195$; FISH: $p < 8.29 \times 10^{-12}$) (Figure 3C); in PV neurons, synaptophysin (*Syp*), an integral membrane protein of small synaptic vesicles associated with the GO term regulation of long-term neuronal synaptic plasticity, is upregulated with age (RNAseq: $p < .026$; FISH: $p < 8.96 \times 10^{-3}$) (Figure 3D); in SST neurons, methyl-CpG binding protein 2 (*Mecp2*), associated with the GO term negative regulation of gene expression, is upregulated with age (RNAseq: $p < .021$; FISH: $p < 1.85 \times 10^{-4}$) (Figure 3E); and in VIP neurons, Arf-GAP with SH3 domain, ANK repeat and PH domain-containing protein 1 (*Asap1*), associated with the GO term dendritic spine morphogenesis, is downregulated with age (RNAseq: $p < 6.83 \times 10^{-5}$; FISH: $p < 2.36 \times 10^{-6}$) (Figure 3F).

Markers of Neuronal Vulnerability Are Differentially Expressed Across Neuronal Subtypes

Neuronal adaptive mechanisms to stress include increased adenosine triphosphate production (thus, higher respiration), increased organelle activity (14), and impaired calcium homeostasis (15), all pathways associated with mitochondria, often at the expense of structural/synaptic homeostasis. In the GO analysis, we observed that interneurons show few changes in pathways associated with these stress-related phenomena compared with PYCs (Figure 3B), suggesting differential vulnerability. Hence, as proxy measures of neuronal vulnerability, we assessed the expression across the four cell types of the *Oxr1* gene, whose product protects against oxidative stress (16), and the *Ryr3* gene, whose product activity depends on the amount of reactive oxygen species present (17,18) (Figure 4A, B). The two genes showed high expression levels in PYC neurons. Highest *Oxr1* expression and lowest *Ryr3* expression was observed in PV neurons. SST neurons displayed intermediate expression profiles between that of PYC and PV neurons, with a slightly lower expression of *Oxr1* but a high expression of *Ryr3*. In contrast, VIP neurons showed low *Oxr1* expression and intermediate *Ryr3* expression. To

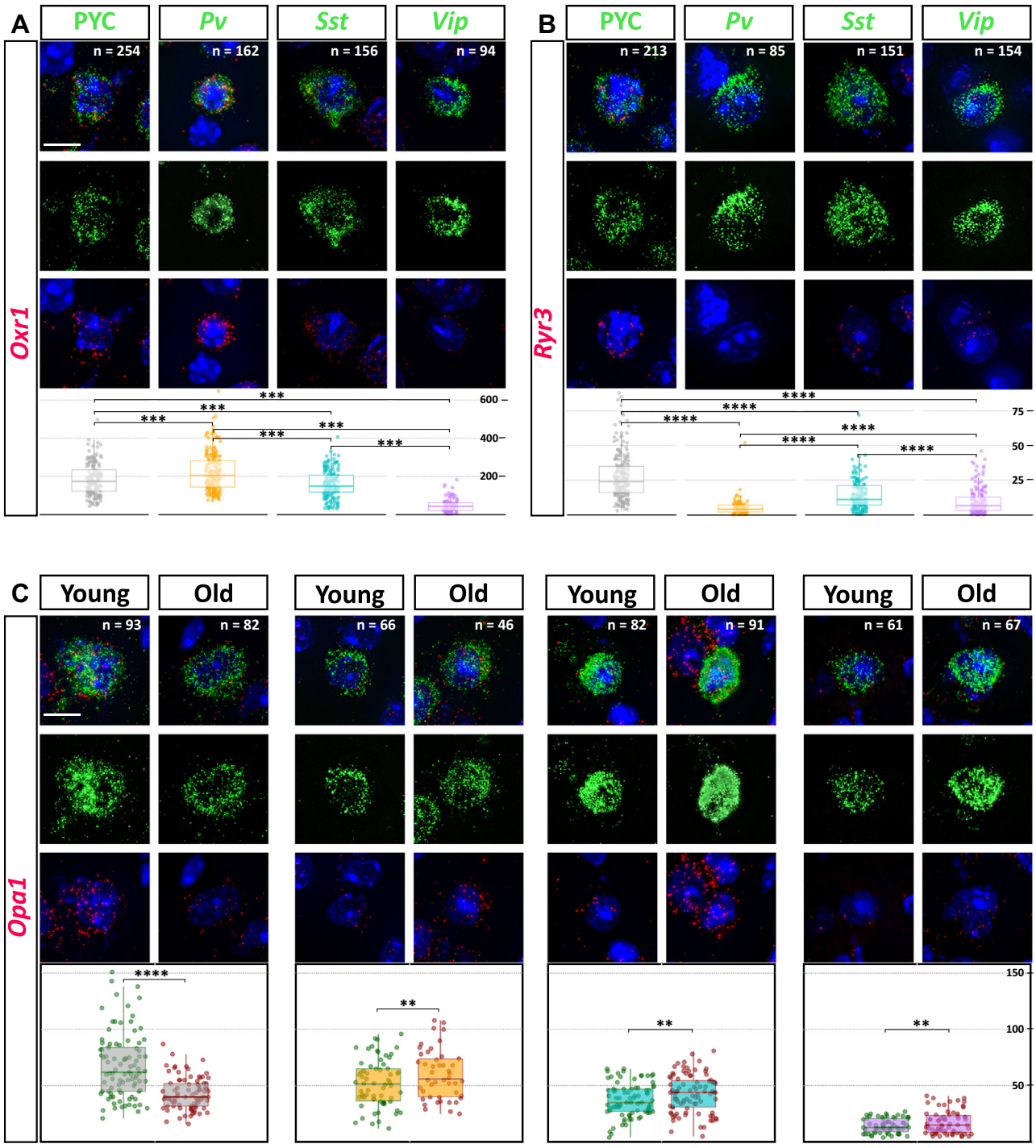

Figure 4. Markers of neuronal vulnerabilities are differentially expressed across cell types. Expression of **(A)** *Oxr1* and **(B)** *Ryr3* messenger RNA (mRNA) across the four cell types, irrespective of age. **(C)** Expression of *Opa1* mRNA changed with age in all neuron types. The expression, with age, is downregulated for pyramidal cells (PYCs), whereas it is upregulated for interneurons. mRNA grains were counted for the differentially expressed gene (red, bottom panel), based on *Slc17a7*, *Pvalb*, *Sst*, and *Vip* cell markers (green, middle panel). The boxplot on the bottom of the figures represents the average mRNA count (*n* [number of cells mentioned in the merged figure]) (top panel). $^{**}p < .01$; $^{***}p < .001$; $^{****}p < .0001$. Scale bar = 10 μm.

complement these measures of cellular vulnerability, we investigated the expression of *Opa1*, a gene upregulated with age exclusively in interneurons (RNAseq, PV: $p < 3.71 \times 10^{-2}$; SST: $p < 3.78 \times 10^{-3}$; VIP: $p < 3.54 \times 10^{-3}$) and whose product is responsible for mitochondrial stability by means of mitochondrial fission-fusion balance (19). As measured by

FISH-quant analysis, *Opa1* expression was high in PYCs, but shows a robust decrease with age in those cells (Figure 4C) (FISH: $p < 5.53 \times 10^{-11}$). Its expression was progressively lower in PV, SST, and VIP neurons, showing small but significant increases with age in all three cell types (FISH, PV: $p < 2.72 \times 10^{-2}$; SST: $p < 1.18 \times 10^{-2}$; VIP: $p < 2.88 \times 10^{-2}$) (Figure 4C), replicating the RNAseq results.

Collectively, the data suggest the following profiles of intrinsic vulnerability and age-associated changes: PYC neurons display an increased vulnerability with age; PV neurons show overall high intrinsic resiliency; SST neurons display moderately high intrinsic resiliency; and VIP displayed low intrinsic resilience. Finally, *Opa1* expression levels suggest that the variability in cellular vulnerability and resilience may be associated with mitochondria-related age-associated changes.

Gene-Behavior Correlation

We performed correlation between gene expression and behavioral dimensions, using individual cognition and anxiety *Z*-scores, and compared results to age-associated changes. As expected, owing to the association of behavioral changes with age, results showed large overlap (Figure 5A). Moreover, because anxiety and cognition *Z*-scores are correlated ($r = .62$), these results suggest that a large group of genes may simultaneously contribute to all three dimensions (age, cognition, and anxiety). To probe for additional and age-independent correlation with behaviors, we performed the same analysis using age-corrected expression profiles. As expected, this reduced the overlap with age-related genes but increased the overlap between cognition- and anxiety-associated genes (Figure 5A), suggesting that a set of gene changes may contribute to both cognition and anxiety changes, independently of aging. We then performed a biological pathway analysis on these age-adjusted and behavior-correlated genes along the same earlier filters for aging to provide direct comparisons. Several observations can be made (Figure 5B). First, results show that, unlike the effect of age, there were minimal upregulated pathways associated with both conditions; changes associated with metabolic pathway were more pronounced in SST and VIP neurons as compared with PYC and PV neurons for both conditions. Second, decreases in pathways related to synaptic structures and channel activity were greatest in PYC neurons and least in VIP neurons. PV neurons showed intermediate and variable results. Up- and downregulated terms in PV neurons were evenly distributed with minimal overlap between the two conditions; however, the number of child terms associated with cognitive decline was twice of that observed in anxiety. PV neurons showed highest

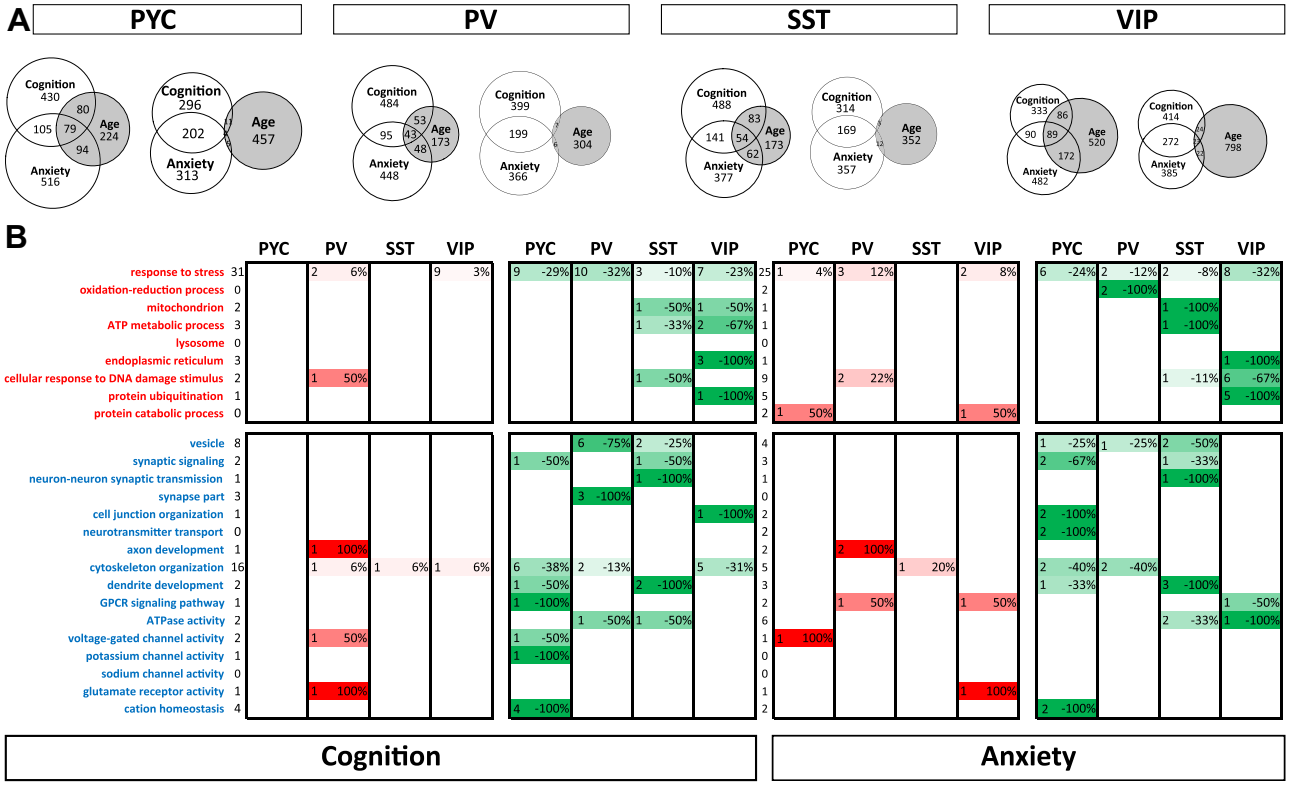

Figure 5. Expression and pathway profile associated with anxiety and cognition. **(A)** Overlap of differentially expressed genes associated with age and *Z*-score of anxiety and cognition with (left) and without (right) age correction for each neuronal subtype. The numbers in the Venn diagram represent the differentially expressed genes (both up- and downregulated). **(B)** Altered pathways related to metabolism and cellular stress (top, red) and synaptic homeostasis and channel activity (bottom, blue) per cell type for anxiety and cognition filtered for parent pathways used for age-associated changes (Figure 3B). Refer to Tables S3 and S4 in Supplement 2 for the detailed parent–child associations with respect to anxiety and cognition, respectively. ATP, adenosine triphosphate; GPCR, G protein–coupled receptor; PV, parvalbumin; PYC, pyramidal cell; SST, somatostatin; VIP, vasoactive intestinal peptide.

upregulated pathways associated with cognitive decline, including glutamate receptor activity, suggesting increased activity of these neurons in relation to cognitive decline. SST neurons showed a very similar and significant number of downregulated metabolic and signaling pathways associated with the two conditions, suggesting a pleiotropic contribution to both increased anxiety and reduced cognition (see summary in Figure 5).

Overall, the results suggest that changes in cognition and anxiety associated with age are partly mediated by normal age-related changes and that age-independent decreases in synaptic and signaling pathways, notably in PYC and SST neurons, contribute more specifically to behavioral changes. Overlaps in pathways suggest that cognition and anxiety associated with age are linked, as suggested by the correlations in anxiety and cognition *Z*-scores, and that SST neurons evenly contribute to both conditions.

DISCUSSION

Assessing age-associated long-term behavioral and cell-specific gene expression changes, we first show that age-associated molecular profiles are unique to each cell type forming cortical microcircuits, with PYCs showing robust metabolic and signaling-related changes. Analysis of intrinsic markers of neuronal vulnerability (*Ryr3*), resilience (*Oxr1*), and mitochondrial dynamics (*Opa1*) further suggests high age-related vulnerability of PYCs and variable degrees of adaptation in GABAergic neurons. Second, we show that age-associated changes in cognition and anxiety largely correlate with normal age-related gene expression changes and that additional age-independent decreases in synaptic and signaling pathways, notably in PYC and SST neurons, may further contribute to behavioral changes. Overlap in findings suggests that age-associated changes in cognition and anxiety are linked, paralleling at the molecular level the correlations in anxiety and cognition behavioral *Z*-scores, and that SST neurons evenly contribute to both conditions. Collectively, the data suggest cell-dependent differential vulnerability and cortical microcircuit-correlated molecular change with age-, anxiety-, and cognition-related changes.

Cells Age Differently

We observed a minimal overlap of age-associated differential expression and biological pathways profile between the four cell types (Figures 2F, G and 3A), suggesting that cells age differently. This was also reflected in the low overlap in affected pathways related to metabolic and synaptic changes (Figure 3B). In PYCs, we observed striking contrast of upregulated metabolic and downregulated synaptic changes, demonstrating an age-related inverse correlation between synaptic structure and metabolic states. PV neurons, more than any other neuronal subtype, showed upregulated synaptic signaling with age. SST neurons showed the highest downregulation of pathways associated with synaptic signaling, consistent with human age-related transcriptomic results (20). Exclusive downregulation of pathways associated with kinase activity was also found in SST neurons. This is consistent with the critical role of kinase activity in inhibitory synapses formation (21,22) and suggests an increased E/I ratio at the microcircuit level, by means of reduced inhibition. This is further supported by increased expression of *Mecp2* (Figure 3E), a marker for E/I balance (8), with age in SST neurons. Finally, VIP neurons showed high similarity and overlap of differentially expressed genes (Figure 2E, F) and functional pathways with PYCs (Figure 3A). The overlapping pathways are associated with excitatory inputs and synaptic communication, suggesting similar excitatory afferent input across the two cell types, consistent with the localization of VIP neurons in layer 1, where PYC distal dendrites are located (23). The input, if lower than expected (in PYCs), will be regulated by the same afferent input to the VIP neurons by means of disinhibition. Supporting this, we also observed greater downregulation in pathways associated with dendrite development in both neuron subtypes with age (Figure 3B), which may suggest an age-associated deafferentiation to these neurons.

Cell Type–Behavior Correlation

At the behavioral level, age-associated increase in anxiety correlates with a decline in cognition (as assessed by working memory), and we show that this is paralleled by large expression changes that do not dissociate between the symptom dimensions and aging. Interestingly, by statistically removing the effect of age on expression, we show that the overlap of genes associated with anxiety and cognition increases (Figure 5A). Thus, even when removing the main effect of age, the biological correlates of anxiety and cognition largely overlap, suggesting a shared biological contribution to both behavioral dimensions. This is consistent with a prior study in human subjects showing that after statistically controlling for various risk factors, the observed age-related reduction in susceptibility to anxiety was associated with decreased emotional responsiveness, increased emotional control, and psychological immunization to stressful experience (24).

At the cell-type level, we observed minimal overlap in specific gene and pathways associated with anxiety or cognition. However, we observed significant overlap between the two behavioral dimensions of changes associated with cellular resources (metabolism) and functionality (synaptic and signaling) for each cell type. This overlap was highest in SST neurons and less in PYC, PV, and VIP neurons. This suggests a non-dissociable role of SST neurons to both behavioral dimensions, relative to the other cell types investigated. This common role of SST neurons may be related to their role in processing specific patterns of information input onto PYCs, common between two highly correlated behaviors (i.e., increased anxiety and reduced cognition), rather than mediating behavioral specificity.

Order of Neuronal Vulnerability

Individual variability in microcircuit cell types during aging suggests the existence of various age-associated vulnerability factors for eventual deficits, whereas, depending on their intrinsic resilience and plasticity, different neuron subtypes may either succumb to or resist these factors. PYCs, in particular, show increased susceptibility to oxidative stress and age-related neurodegenerative disorders (14), whereas some interneuron subtypes may be relatively resilient (25). This may relate to the presence of glutamate decarboxylase (GAD) and calbindin-binding protein, known for their

neuroprotective properties (25,26). Consistent with these observations, we show that expression of *Opa1* is enriched with age in interneurons but not in PYCs. OPA1 is a guanosine triphosphate enzyme protein found in the inner mitochondrial membrane that facilitates mitochondria fusion, oxidative phosphorylation, adenosine triphosphate levels, and mitochondria Ca^{2+} retention (27), together implying that mitochondrial homeostasis may contribute to interneuron resilience. In PYCs, confirming its most vulnerable status, we also observed highest expression of *Ryr3*, a marker of reactive oxygen species turnover (14).

PV neurons are enwrapped with a specialized polyanionic matrix called perineuronal nets, which protect from oxidative stress (28). This net also permits the capture and accumulation of *Otx2* hemoprotein, which provides plasticity to mature PV neurons (29). The current results further support a resiliency mechanism for PV neurons: 1) the overall expression of GAD (GAD1 + GAD2), an enzyme with neuroprotective role, was significantly higher in PV neurons compared with other interneurons (Figure 2D); 2) pathways associated with synaptic signaling were upregulated with age in PV neurons to a greater extent than in any other neuron (Figure 3B); and 3) PV neurons displayed the highest *Oxr1* expression (Figure 4A), a marker for neuroprotection, and the lowest expression of *Ryr3* (Figure 4B), a marker for reactive oxygen species turnover. These observations are in a stark contrast with PYCs, positioning the two neuronal subtypes at opposite ends of the vulnerability scale. SST and VIP neurons display intermediate vulnerability levels, with VIP neurons sharing similarities in expression profiles and vulnerability markers with PYCs. This putative order of vulnerability has implications for disease mechanisms, as an accelerated age-related molecular profile may represent sources of pathophysiology for brain disorders (30). For instance, age-related changes in SST neurons have been reported across diseases (31). However, the current results suggest that age- and disease-related changes in SST neurons gene expression profiles may have distinct biological origins and contributions to behavioral dimensions. Finally, this study of healthy aging suggests a high resiliency of PV neurons, whereas there are reports of PV neurons vulnerability in many forms of mental illness (28). This suggests that the age-related neuronal vulnerabilities may not necessarily translate into vulnerability to disease processes.

Limitations

First, owing to its higher cell density, some technical noise is expected when collecting PYCs, compared with interneurons using LCM. Second, our main aim was to determine transcriptomic changes in cell types forming the canonical cortical microcircuitry, and we did not collect layer-specific cell types. Third, we used a targeted LCM approach to collect pools of similar cells rather than a single-cell RNAseq approach. This provides greater sequencing depth per cell type but misses the finer dissociation of cell types. Finally, this study was performed in male mice, due to the availability only of aged male mice at the time of the study, and focused only on the frontal cortex, for its association with the behavioral tasks we performed. Assessing additional behavioral tasks, sex, and area differences in age-related cell-type aging will provide further information on cell-specific biological vulnerability relating to age.

ACKNOWLEDGMENTS AND DISCLOSURES

This work was supported by Canadian Institute of Health Research Project Grant No. 153175 (to ES), National Alliance for Research on Schizophrenia and Depression award Grant No. 25637 (to ES) and National Institute of Mental Health Grant No. R01 MH093723 (to ES).

We thank Keith Misquitta for help with the behavioral assays and the Centre for Addiction and Mental Health Sequencing Facility for help in running the Illumina Sequencing Platform.

The authors report no biomedical financial interests or potential conflicts of interest.

ARTICLE INFORMATION

From the Campbell Family Mental Health Research Institute (RS, TDP, LF, BRR, MB, ES) and Krembil Centre for Neuroinformatics (LF), Centre for Addiction and Mental Health; and the Department of Psychiatry (RS, LF, MB, ES), Donnelly Center for Cellular and Biomolecular Research (RI, GDB), Departments of Pharmacology and Toxicology (MB, ES), and Institute of Medical Science (LF, ES), University of Toronto, Toronto, Canada.

Address correspondence to Etienne Sibille, Ph.D., Campbell Family Mental Health Research Institute of CAMH, Department of Psychiatry, 250 College St, Room 134, Toronto, ON M5T 1R8, Canada; E-mail: Etienne.Sibille@camh.ca.

Received Jun 14, 2018; revised Aug 30, 2018; accepted Sep 11, 2018.

Supplementary material cited in this article is available online at https://doi.org/10.1016/j.biopsych.2018.09.019.

REFERENCES

1. Dickstein DL, Kabaso D, Rocher AB, Luebke JI, Wearne SL, Hof PR (2007): Changes in the structural complexity of the aged brain. Aging Cell 6:275–284.
2. Bonifazi P, Goldin M, Picardo MA, Jorquera I, Cattani A, Bianconi G, *et al.* (2009): GABAergic hub neurons orchestrate synchrony in developing hippocampal networks. Science 326:1419–1424.
3. Fee C, Banasr M, Sibille E (2017): Somatostatin-positive gamma-aminobutyric acid interneuron deficits in depression: Cortical microcircuit and therapeutic perspectives. Biol Psychiatry 82:549–559.
4. Isaacson JS, Scanziani M (2011): How inhibition shapes cortical activity. Neuron 72:231–243.
5. Nelson SB, Valakh V (2015): Excitatory/inhibitory balance and circuit homeostasis in autism spectrum disorders. Neuron 87:684–698.
6. Segovia G, Porras A, Del Arco A, Mora F (2001): Glutamatergic neurotransmission in aging: A critical perspective. Mech Ageing Dev 122:1–29.
7. Porges EC, Woods AJ, Edden RAE, Puts NAJ, Harris AD, Chen H, *et al.* (2017): Frontal gamma-aminobutyric acid concentrations are associated with cognitive performance in older adults. Biol Psychiatry Cogn Neurosci Neuroimaging 2:38–44.
8. Lee E, Lee J, Kim E (2017): Excitation/inhibition imbalance in animal models of autism spectrum disorders. Biol Psychiatry 81:838–847.
9. Rozycka A, Liguz-Lecznar M (2017): The space where aging acts: Focus on the GABAergic synapse. Aging Cell 16:634–643.
10. Love MI, Huber W, Anders S (2014): Moderated estimation of fold change and dispersion for RNA-seq data with DESeq2. Genome Biol 15:550.
11. Subramanian A, Tamayo P, Mootha VK, Mukherjee S, Ebert BL, Gillette MA, *et al.* (2005): Gene set enrichment analysis: A knowledge-based approach for interpreting genome-wide expression profiles. Proc Natl Acad Sci U S A 102:15545–15550.
12. Mueller F, Senecal A, Tantale K, Marie-Nelly H, Ly N, Collin O, *et al.* (2013): FISH-quant: Automatic counting of transcripts in 3D FISH images. Nat Methods 10:277–278.
13. Gene Ontology Consortium (2004): The Gene Ontology (GO) database and informatics resource Nucleic Acids Res 32:D258–D261.

14. Wang X, Michaelis EK (2010): Selective neuronal vulnerability to oxidative stress in the brain. Front Aging Neurosci 2:12.
15. Nikoletopoulou V, Tavernarakis N (2012): Calcium homeostasis in aging neurons. Front Genet 3:200.
16. Oliver PL, Finelli MJ, Edwards B, Bitoun E, Butts DL, Becker EBE, *et al.* (2011): Oxr1 Is essential for protection against oxidative stress-induced neurodegeneration. PLoS Genet 7:e1002338.
17. Vervliet T, Lemmens I, Vandermarliere E, Decrock E, Ivanova H, Monaco G, *et al.* (2015): Ryanodine receptors are targeted by anti-apoptotic Bcl-XL involving its BH4 domain and Lys87 from its BH3 domain. Sci Rep 5:9641.
18. Marengo JJ, Hidalgo C, Bull R (1998): Sulfhydryl oxidation modifies the calcium dependence of ryanodine-sensitive calcium channels of excitable cells. Biophys J 74:1263–1277.
19. Bertholet AM, Millet AME, Guillermin O, Daloyau M, Davezac N, Miquel M-C, Belenguer P (2013): OPA1 loss of function affects in vitro neuronal maturation. Brain 136:1518–1533.
20. French L, Ma T, Oh H, Tseng GC, Sibille E (2017): Age-related gene expression in the frontal cortex suggests synaptic function changes in specific inhibitory neuron subtypes. Front Aging Neurosci 9:162.
21. Kuroda Y, Ichikawa M, Muramoto K, Kobayashi K, Matsuda Y, Ogura A, Kudo Y (1992): Block of synapse formation between cerebral cortical neurons by a protein kinase inhibitor. Neurosci Lett 135: 255–258.
22. Flores CE, Nikonenko I, Mendez P, Fritschy J-M, Tyagarajan SK, Muller D (2015): Activity-dependent inhibitory synapse remodeling through gephyrin phosphorylation. Proc Natl Acad Sci U S A 112: E65–E72.
23. Pi H-J, Hangya B, Kvitsiani D, Sanders JI, Huang ZJ, Kepecs A (2013): Cortical interneurons that specialize in disinhibitory control. Nature 503:521–524.
24. Jorm AF (2000): Does old age reduce the risk of anxiety and depression? A review of epidemiological studies across the adult life span. Psychol Med 30:11–22.
25. Mattson MP, Magnus T (2006): Ageing and neuronal vulnerability. Nat Rev Neurosci 7:278–294.
26. Lewis NE, Schramm G, Bordbar A, Schellenberger J, Andersen MP, Cheng JK, *et al.* (2010): Large-scale in silico modeling of metabolic interactions between cell types in the human brain. Nat Biotechnol 28:1279–1285.
27. Kushnareva YE, Gerencser AA, Bossy B, Ju WK, White AD, Waggoner J, *et al.* (2013): Loss of OPA1 disturbs cellular calcium homeostasis and sensitizes for excitotoxicity. Cell Death Differ 20:353–365.
28. Cabungcal J-H, Steullet P, Morishita H, Kraftsik R, Cuenod M, Hensch TK, Do KQ (2013): Perineuronal nets protect fast-spiking interneurons against oxidative stress. Proc Natl Acad Sci 110:9130–9135.
29. Beurdeley M, Spatazza J, Lee HHC, Sugiyama S, Bernard C, Di Nardo AA, *et al.* (2012): Otx2 binding to perineuronal nets persistently regulates plasticity in the mature visual cortex. J Neurosci 32: 9429–9437.
30. McKinney BC, Sibille E (2013): The age-by-disease interaction hypothesis of late-life depression. Am J Geriatr Psychiatry 21:418–432.
31. Sibille E (2013): Molecular aging of the brain, neuroplasticity, and vulnerability to depression and other brain-related disorders. Dialogues Clin Neurosci 15:53–65.